THE JOURNAL OF BIOLOGICAL CHEMISTRY
Vol. 280, No. 19, Issue of May 13, pp. 19078–19086, 2005

Printed in U.S.A.

The Benzo[*c*]phenanthridine Alkaloid, Sanguinarine, Is a Selective, Cell-active Inhibitor of Mitogen-activated Protein Kinase Phosphatase-1*

Received for publication, February 8, 2005
Published, JBC Papers in Press, March 7, 2005, DOI 10.1074/jbc.M501467200

Andreas Vogt‡, Aletheia Tamewitz, John Skoko, Rachel P. Sikorski, Kenneth A. Giuliano§, and John S. Lazo¶

From the Department of Pharmacology, University of Pittsburgh, Pittsburgh, Pennsylvania 15261

Mitogen-activated protein kinase phosphatase-1 (MKP-1) is a dual specificity phosphatase that is overexpressed in many human tumors and can protect cells from apoptosis caused by DNA-damaging agents or cellular stress. Small molecule inhibitors of MKP-1 have not been reported, in part because of the lack of structural guidance for inhibitor design and definitive assays for MKP-1 inhibition in intact cells. Herein we have exploited a high content chemical complementation assay to analyze a diverse collection of pure natural products for cellular MKP-1 inhibition. Using two-dimensional Kolmogorov-Smirnov statistics, we identified sanguinarine, a plant alkaloid with known antibiotic and antitumor activity but no primary cellular target, as a potent and selective inhibitor of MKP-1. Sanguinarine inhibited cellular MKP-1 with an IC_{50} of 10 μM and showed selectivity for MKP-1 over MKP-3. Sanguinarine also inhibited MKP-1 and the MKP-1 like phosphatase, MKP-L, *in vitro* with IC_{50} values of 17.3 and 12.5 μM, respectively, and showed 5–10-fold selectivity for MKP-3 and MKP-1 over VH-1-related phosphatase, $Cdc25B_2$, or protein-tyrosine phosphatase 1B. In a human tumor cell line with high MKP-1 levels, sanguinarine caused enhanced ERK and JNK/SAPK phosphorylation. A close congener of sanguinarine, chelerythrine, also inhibited MKP-1 *in vitro* and in whole cells, and activated ERK and JNK/SAPK. In contrast, sanguinarine analogs lacking the benzophenanthridine scaffold did not inhibit MKP-1 *in vitro* or in cells nor did they cause ERK or JNK/SAPK phosphorylation. These data illustrate the utility of a chemical complementation assay linked with multiparameter high content cellular screening.

Mitogen-activated protein kinase phosphatase (MKP)[1]-1 is a dual specificity phosphatase that is overexpressed in many human tumors and protects cells from apoptosis by the anticancer agent cisplatin (1), UV irradiation (2), and proteasome inhibitors (3). Over the past five years, reports have become more numerous describing high levels of MKP-1 in human tumors. For example, high levels of MKP-1 have been found in prostate (4), gastric (5), breast (6), and pancreatic cancer (7). In ovarian cancer samples, MKP-1 expression was correlated with decreased progression-free survival (8). High levels of MKP-1 expression were also found in the early phases of prostate, colon, and bladder carcinogenesis (9). Evidence that MKP-1 may actually support the transformed phenotype comes from a recent study by Liao *et al.* (7) who showed that PANC-1 human pancreatic cancer cells stably transfected with a full-length MKP-1 antisense construct had longer doubling times, decreased ability to form colonies in soft agar, and were unable to form tumors in nude mice. The precise mechanism by which loss of MKP-1 expression affects tumorigenicity, however, remains elusive. Several reports have implicated JNK/SAPK and p38 as the primary mediators of MKP-1 mediated cytoprotection (1–2). On the other hand, the data presented by Liao *et al.* (7) argue that the primary mechanism by which MKP-1 supports the transformed phenotype is mediated by ERK, but not JNK, as suppression of MKP-1 expression by antisense did not affect basal levels of phospho-JNK or phospho-p38, but instead increased basal ERK phosphorylation and prolonged ERK phosphorylation after epidermal growth factor stimulation in PANC-1 cells.

The availability of a cell-active selective MKP-1 inhibitor would be a valuable tool for dissecting the complex regulatory processes involved in the attenuation of ERK, JNK, and p38 activation and for defining the contributions of MKP-1 and its cellular targets to the maintenance of the transformed phenotype. In light of recent findings, inhibitors of MKP-1 might also find applications as novel target-based antineoplastic therapies, either alone or in combination with clinically used antineoplastic agents (1–3).

The search for MKP-1 inhibitors has been challenging for several reasons. In contrast to MKP-3, whose crystal structure has been reported and found to possess high structural similarity to the related VHR in its catalytic domain (10), no structural information is available for MKP-1. This may in part be due to difficulties in producing large amounts of recombinant enzyme and the need of MKPs to interact with their physiolog-

* This work was supported by National Institutes of Health Grants CA78039 and CA52995 and the Fiske Drug Discovery Fund. The costs of publication of this article were defrayed in part by the payment of page charges. This article must therefore be hereby marked "*advertisement*" in accordance with 18 U.S.C. Section 1734 solely to indicate this fact.

‡ To whom correspondence may be addressed: Dept. of Pharmacology, The Hillman Cancer Center G.27a, University of Pittsburgh, Pittsburgh, PA 15213. Tel.: 412-623-1216; Fax: 412-623-1212; E-mail: avogt@pitt.edu.

§ Current address: Cellumen, Inc., 100 Technology Dr., Pittsburgh, PA 15219.

¶ To whom correspondence may be addressed: Dept. of Pharmacology, Biomedical Science Tower E-1340, University of Pittsburgh, Pittsburgh, PA 15261. Tel.: 412-648-9319; Fax: 412-648-2229; E-mail: lazo@pitt.edu.

[1] The abbreviations used are: MKP, mitogen-activated protein kinase phosphatase; ERK, extracellular signal regulated kinase; FITC, fluorescein isothiocyanate; GFP, green fluorescent protein; GST, glutathione *S*-transferase; HCS, high content screening; JNK/SAPK, c-Jun terminal kinase/stress-activated protein kinase; KS, Kolmogorov-Smirnov; MAPK, mitogen-activated protein kinase; PAO, phenylarsine oxide; pERK, phospho-ERK; TPA, 12-*O*-tetradecanoylphorbol 13-acetate; VHR, VH-1 related phosphatase.

ical substrates to become fully active (11). The conformational changes associated with phosphatase-substrate interactions may render assays based on dephosphorylation of small molecule substrates or short peptides inaccurate predictors of effective phosphatase inhibitors in a physiological context.

Cellular assays provide a potentially powerful alternative to *in vitro* screening for phosphatase inhibitors. The advent and maturation of cellular assay technologies such as high content screening (HCS) (12) permit the construction of rapid and quantitative discovery assays with definitive phenotypic endpoints. In this report, we have combined a definitive cellular assay for MKP-1 activity with HCS methodology and an unbiased statistical analysis of the HCS data set, and executed a small molecule screen for inhibitors of MKP-1 in intact mammalian cells. By analyzing a relatively small number of diverse natural products, we identified a plant alkaloid, sanguinarine, as a cell-active inhibitor of MKP-1. Compound credentialing was greatly facilitated by the employment of a cellular assay, which selected compounds with a defined biological activity. These results not only reveal sanguinarine as the first reported selective inhibitor of MKP-1 but also expose a primary cellular target for some of the biological activities of sanguinarine.

MATERIALS AND METHODS

Compounds—The MicroSource Natural Products Library (Discovery Systems, Inc., Gaylordsville, CT) is a 720-compound collection of pure natural products and their derivatives. The collection includes simple and complex oxygen heterocycles, alkaloids, sesquiterpenes, diterpenes, pentacyclic triterpenes, sterols, and many other diverse representatives. Compounds were supplied as 10 mM stocks of Me_2SO, stored at −20 °C and thawed immediately before analysis. Aliquots were dissolved to a final concentration of 50 μM in complete growth medium prior to cell treatment. Lipofectamine 2000 was from Invitrogen. All other chemicals, including the sanguinarine analogs, were purchased from Sigma-Aldrich.

Antibodies and Plasmids—Mouse monoclonal anti-phospho-ERK (E10), rabbit polyclonal phospho-ERK, phospho-JNK, and pan-JNK/SAPK antibodies were from Cell Signaling Technology (Beverly, MA). Rabbit polyclonal ERK antibody and mouse monoclonal anti-c-myc (9E10) antibodies were from Santa Cruz Biotechnology (Santa Cruz, CA). Secondary antibodies were AlexaFluor 488-conjugated goat anti-mouse, AlexaFluor 546-, 555-, and 647-conjugated anti-rabbit IgG (Molecular Probes, Eugene, OR), and horseradish peroxidase-conjugated goat-anti rabbit IgG and goat-anti mouse IgG (Jackson ImmunoResearch, West Grove, PA). cDNA encoding myc-tagged human MKP-3 (PYST-1) in a pSG5 mammalian expression vector (37, 38) and CL100 in a pET15b bacterial expression vector were gifts from Dr. Stephen Keyse (CRUK, Dundee, UK). A plasmid encoding myc-tagged mouse MKP-1 in a pCEP4 mammalian expression vector was a gift from Dr. Nicholas Tonks (Cold Spring Harbor Laboratories). To improve transfection efficiency, a BamH1 fragment containing the c-myc-MKP-1 sequence was excised from the pCEP4 vector and subcloned into pcDNA3.1 (Clontech). Bacterial expression vectors for human His_6-MKP-3 and His_6-MKP-1 were gifts from Dr. Zhong-Yin Zhang (Albert Einstein College of Medicine, Bronx, NY) and Dr. Jack Dixon, (University of California, San Diego, CA), respectively. The pEGFP-C1 expression vector was from Clontech. The identities of all cDNA constructs were verified by sequencing.

Cell Culture—PANC-1 and HeLa cells were obtained from ATCC (Manassas, VA), and were maintained in Dulbecco's minimum essential medium containing 10% fetal bovine serum (HyClone, Logan, UT), and 1% penicillin-streptomycin (Invitrogen) in a humidified atmosphere of 5% CO_2 at 37 °C.

High Content Screening for MKP-1 Inhibitors—HeLa cells (5,000) were plated in the wells of collagen-coated 384-well plates (Falcon Biocoat) and allowed to attach overnight. Cells were transfected with c-myc-MKP-1 or EGFP cDNAs (100 ng/well) and Lipofectamine 2000 (2.5 μl/μg DNA) in Opti-MEM-reduced serum medium as per manufacturer's instructions. Three hours after transfection, complexes were removed and fresh medium containing 10% fetal bovine serum was added. Eighteen hours later, cells were treated in duplicate wells for 15 min with TPA or mixtures of TPA and library compounds, fixed and immunostained with a mixture of anti-phospho-ERK (1:200 dilution) and anti-c-myc (1:100 dilution) antibodies as described (14). Positive phospho-ERK and c-myc-MKP-1 signals were visualized with AlexaFluor 647 (phospho-ERK) and AlexaFluor 488-(c-myc)-conjugated secondary antibodies, respectively. All staining steps were carried out on a Biomek 2000 laboratory automation work station (Beckman-Coulter, Inc., Fullerton, CA). For confirmatory and selectivity studies, cells were transfected with MKP-1, MKP-3, or GFP, using 4–12 wells for each treatment condition. In some cases, phospho-ERK was visualized using AlexaFluor 546 or AlexaFluor 555 secondary antibodies.

Plates were analyzed by three-channel multiparametric analysis for phospho-ERK and c-myc-MKP intensities in an area defined by nuclear staining using the Compartmental Analysis Bioapplication on the ArrayScan II (Cellomics, Pittsburgh, PA). Images were acquired in three independent fluorescence channels using an Omega XF93 filter set at excitation/emission wavelengths of 350/461 nm (Hoechst), 494/519 nm (AlexaFluor 488), 556/573 nm (AlexaFluor 546/555), or 650/665 nm (AlexaFluor 647), respectively. At least 1,000 individual cells were analyzed for phospho-ERK, c-myc-MKP-3, c-myc-MKP-1, or GFP intensities. For each condition, the percentage of MKP (GFP)-expressing cells was determined from FITC (AlexaFluor 488) intensity distribution histograms, setting appropriate gates for MKP (GFP)-positive and MKP (GFP)-negative cells.

Analysis of HCS Data: Generalization of the Kolmogorov-Smirnov Test to Two-dimensional Data Distributions—The one-dimensional Kolmogorov-Smirnov (KS) test was adapted to two dimensions by Ref. 20 and further refined by Ref. 21. The approach used here was a modification of the Fortran 77 implementation of the above work (39). Briefly, the two-dimensional data distributions representing two physiological parameters from a multiparameter HCS assay obtained after drug treatment were compared with the two-dimensional data distributions obtained from multiple wells of untreated cells. First, each data distribution was divided into quadrants defined by the median x and y axis values calculated from the untreated cell data distributions. The two-dimensional KS statistic was then found by ranging through all four quadrants to find the maximal difference between the fraction of cells in each treated quadrant and the fraction of cells in each corresponding untreated quadrant. Calculations were performed with the S-Plus statistical software package (Insightful, Inc., Seattle, WA).

Analysis of HCS Data: Percent Responder Analysis—MKP-expressing and non-expressing cell populations were gated as above. A threshold for phospho-ERK-positive cells was defined as the average Cy5 intensity + 2 standard deviations from a randomly chosen, MKP-1-transfected well, and the percentage of cells in the MKP-1 (GFP)-expressing cell subpopulations whose pERK staining intensities exceeded the pERK threshold was calculated. Using this method, the percentage of phospho-ERK-positive cells was low (<5%) in MKP-1-expressing cells, and high (up to 90%) in GFP-expressing cells (see Fig. 4).

In Vitro Phosphatase Assays—Full-length MKP-3, and Cdc25B2 as well as the catalytic domain of Cdc25B2 were expressed as His_6-tagged fusion proteins from pET21a vectors. Full-length VHR and protein-tyrosine phosphatase 1B were expressed as GST fusion proteins from a pGEX2T vector as described (40). GST and His_6-tagged fusion proteins were purified from *Escherichia coli* using standard methodology. His-tagged human MKP-1 (CL100) was expressed from a pET15b vector and purified on Talon resin. Phosphatase activity assays were performed using a fluorescence-based 96-well microtiter plate assay with *O*-methyl fluorescein phosphate (OMFP) as previously described (40, 41). Inhibition studies were conducted at optimal pH using OMFP at its K_m value for each phosphatase.

Simultaneous Measurement of Phospho-ERK and Phospho-JNK Levels by Quantitative Immunofluorescence Microscopy—PANC-1 cells (10,000/well) were plated in the wells of a 384-well microplate, allowed to attach overnight, and treated for 30 min with vehicle (Me_2SO), TPA (500 ng/ml), anisomycin (25 μg/ml), phenylarsine oxide (PAO) (5 μM), or unknown compounds. Cells were fixed and immunostained with a mixture of anti-phospho-ERK (E10 mouse monoclonal) and anti-phospho-JNK (rabbit polyclonal) antibodies (1:200 dilution), followed by incubation with AlexaFluor 488-conjugated goat anti-mouse IgG and AlexaFluor 647-conjugated goat anti-rabbit IgG. Nuclei were counterstained with Hoechst 33342 and average nuclear AlexaFluor 488 and AlexaFluor 647 fluorescence intensities were measured on the ArrayScan II in an area defined by the nucleus, as described above. To control for potential compound autofluorescence, background fluorescence values were measured for each condition in the absence of primary antibodies and subtracted from the average fluorescence intensities obtained in the presence of primary antibodies.

Western Blotting—PANC-1 cells (1.5×10^6) were plated in 100-mm tissue culture dishes, exposed to compounds for 30 min, harvested by

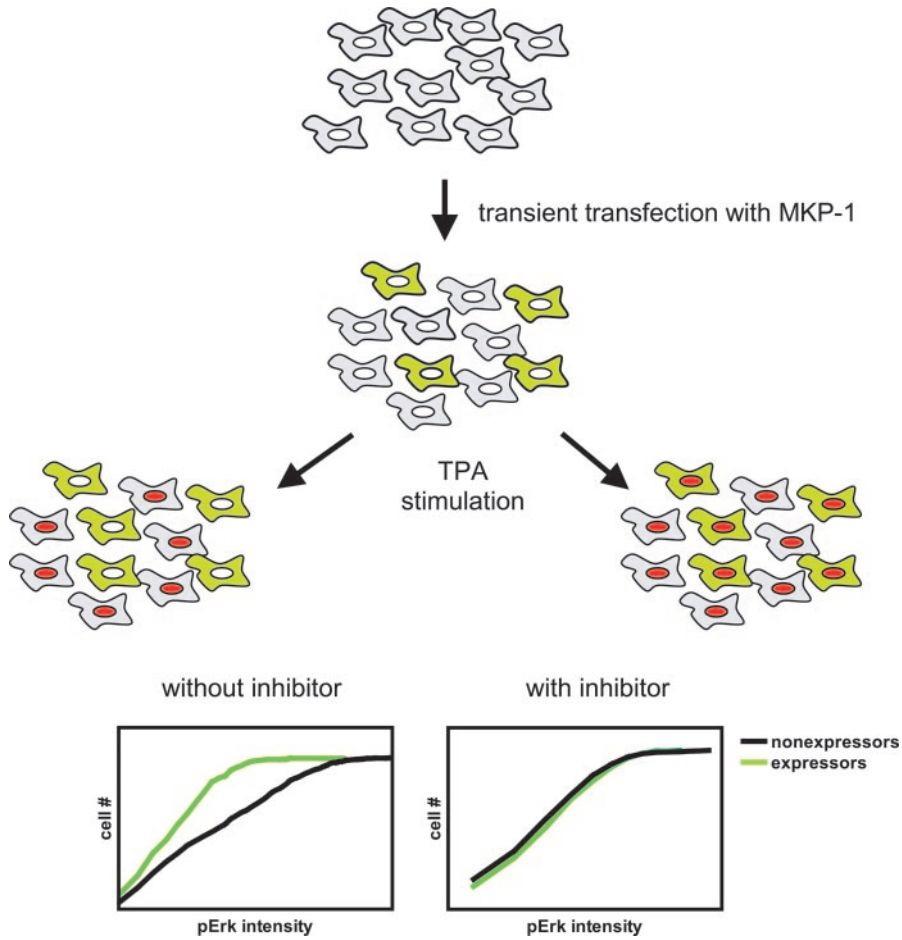

FIG. 1. **Schematic representation of a high content chemical complementation assay in intact mammalian cells.** Cells are transfected in multiwell plates with plasmids encoding the MKP-1 phosphatase, resulting in target expression in a subpopulation of transfected cells (shown in *green*). Upon stimulation, the non-expressing cells respond with enhanced nuclear accumulation of phospho-ERK (*red*), whereas MKP-1-expressing cells do not. Inclusion of an MKP inhibitor restores phospho-ERK levels in the nucleus of MKP-expressing cells to that seen in non-expressing cells. Differences in nuclear phospho-ERK levels between the two subpopulations can be quantified as a measure of MKP activity.

trypsinization, and lysed. Cell lysates were resolved on 4–20% SDS-polyacrylamide gels and transferred to nitrocellulose membranes (Protran, Schleicher & Schuell). Membranes were probed with anti-phospho-ERK, phospho-JNK, anti-ERK, and anti-JNK antibodies. Positive antibody reactions were visualized using peroxidase-conjugated secondary antibodies (Jackson ImmunoResearch, West Grove, PA) and an enhanced chemiluminescence detection system (Western Lightning, PerkinElmer Life Sciences) according to manufacturer's instructions. For quantitation of protein expression levels, luminescence band intensities were measured on a Kodak i1000 imaging station using a 14-bit CCD camera under non-saturating conditions (PerkinElmer Life Sciences).

RESULTS

High Content Screening of a Natural Products Library Using a Definitive Assay for MKP-1 Activity in Intact Cells—We implemented a definitive assay for MKP-1 inhibition in intact mammalian cells as a high content cellular screen. The fundamental approach, which we have termed "chemical complementation" (13) and recently implemented for high content screening (14), is based on the measurement of ERK phosphorylation in MKP-1 expressing and non-expressing cell subpopulations after transient transfection with mammalian expression plasmids, similar to that previously used to credential inhibitors of MKP-3 (14) (Fig. 1). HeLa cells were plated in 384-well plates and transiently transfected with a mammalian expression plasmid encoding c-myc-tagged MKP-1. Twenty one hours after transfection, cells were stimulated with TPA to generate a strong and uniform phospho-ERK signal, and immunostained with a mixture of anti-c-myc and anti-phospho-ERK antibodies. c-myc-MKP-1 and pERK-positive cells were visualized with AlexaFluor 488 and AlexaFluor 647 secondary antibodies, respectively. Using this methodology, immunofluorescence images showed that MKP-1-expressing cells had low levels of phospho-ERK compared with surrounding non-expressing cells (see Fig. 3 for a representative example).

We then screened 720 members of a commercially available natural products library for compounds that restored phospho-ERK levels in the MKP-1 expressing cells to that seen in non-expressing cells. Each microplate contained four wells with untransfected cells, four wells each with cells transfected with empty vector or GFP, 16 wells with cells transfected with MKP-1 and treated with vehicle, and 160 wells with cells transfected with MKP-1 and treated with library compounds. All wells were stimulated for 15 min with TPA alone or TPA in combination with library compounds in duplicate at a single concentration of 50 μM. The broad protein-tyrosine phosphatase inhibitor, PAO, was included as a positive control. A minimum of 1,000 individual cells in each well were then analyzed on an ArrayScan II for c-myc and phospho-ERK intensities, and gated into c-myc-MKP-1 expressing and non-expressing cell subpopulations by setting a threshold for c-myc immunoreactivity based on the AlexaFluor 488 intensity of mock-transfected wells. This procedure yielded an HCS data set containing individual channel intensities for each individual cell that was used to determine transfection efficiencies and phospho-ERK levels. Consistent with our previous report, we found transfection efficiencies of up to 30% for MKP-1 and up to 55% for GFP, which was included as positive control.

Identification of Positives—To identify positive compounds, we used a two-dimensional KS analysis with the HS data set. KS statistics have been described as a method to quantitatively compare the distributions of individual cell populations (15–18), and shown to be a valuable tool for the quantification of HCS data (19). The two-dimensional KS method ranges over data in a (x, y) plane in search of a maximum cumulative

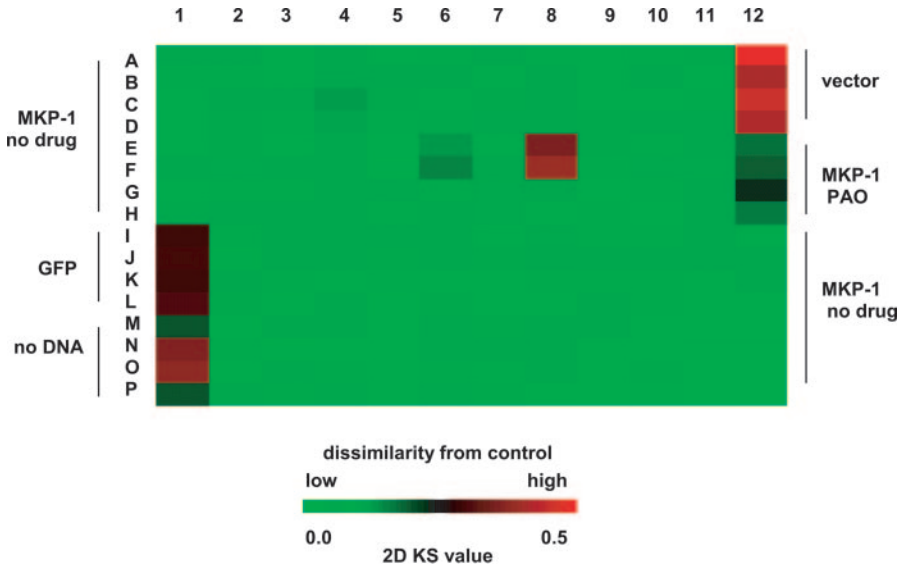

FIG. 2. **Two-dimensional KS statistics and representative plate from the screen.** HeLa cells were transfected with MKP-1 or GFP, stimulated for 15 min with TPA in the presence or absence of library compounds, and analyzed for MKP-1 expression and phospho-ERK levels in the FITC and Cy5 channels, respectively, as described under "Materials and Methods." A representative plate layout is shown. Each plate contained 16 wells of vehicle-treated cells, 4 wells each of GFP, mock-transfected cells, four wells of cells transfected with MKP-1 and treated with the positive control, PAO, and 80 library compounds in duplicate. Data were analyzed by two-dimensional KS statistics as described under "Materials and Methods." Individual *rectangles* represent wells that were color-coded based on two-dimensional Kolmogorov-Smirnov statistics obtained from comparing the population distributions of each well to that of MKP-1-transfected and vehicle-treated control wells. *Green* and *red rectangles* represent low and high dissimilarity values compared with control. Wells *E8* and *F8* contain the positive compound from the HCS screen, sanguinarine.

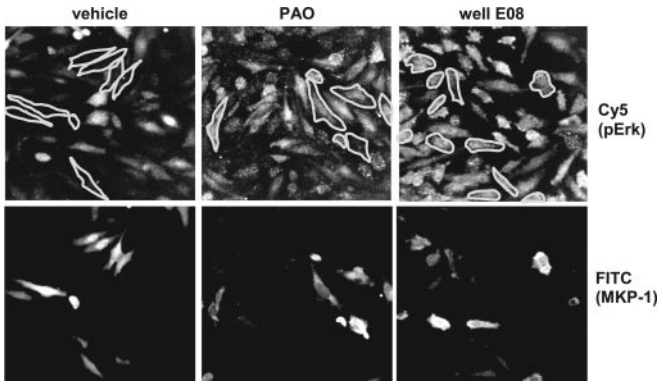

FIG. 3. **Visual confirmation of the positive compound identified in the natural products library.** Archived immunofluorescence images from the MKP-1 high content screen were manually evaluated for c-myc-MKP-1 and phospho-ERK (*pERK*) expression. MKP-1-transfected and TPA-stimulated HeLa cells were simultaneously immunostained for c-myc-MKP-1 (*lower panel*) and phospho-ERK (*upper panel*). Images shown are representative fields from wells treated with vehicle (Me_2SO), PAO, or sanguinarine sulfate from the microsource library (*well E08*). MKP-1-expressing cells (*lower panel*) were visually identified and traced, and traces were transferred to Cy5 channel images (*upper panel*). MKP-1 reduces phospho-ERK levels in MKP-1-expressing cells. Both PAO and sanguinarine restored phospho-ERK in MKP-1-expressing cells.

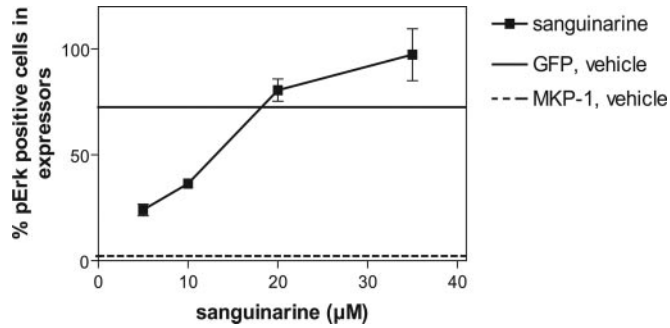

FIG. 4. **Concentration-dependent inhibition of MKP-1 in intact cells by sanguinarine.** HeLa cells transfected with c-myc-MKP-1 or c-myc-MKP-3 were stimulated with TPA in the presence of various concentrations of sanguinarine. Cells were gated into MKP-expressing and non-expressing subpopulations based on green fluorescence intensity and into phospho-ERK-positive and -negative subpopulations based on Cy5 fluorescence intensity as described in the Methods section. The *solid* and *dashed lines* denote the percentage of phospho-ERK-positive cells in vehicle-treated, GFP, and MKP-1-expressing cells, respectively. Data are the average percentage of phospho-ERK-positive cells in the MKP-1 (GFP)-expressing cell subpopulations from 8 wells ± S.E. from a single experiment that has been repeated with similar results.

difference between two two-dimensional data distributions (20–21). The resulting KS values can assume a value between 0 (identical distributions) and 1 (completely different distributions). To fully exploit the information contained in our multiparameter high content data, we developed an algorithm that combined the KS statistics with ratio analysis of means (17) of both AlexaFluor 488 (MKP-1) and AlexaFluor 647 (phospho-ERK) in a minimum of 1,000 individual cells in 192 wells on a 384-well microplate. Two color fluorescence data from 16 controls (MKP-1 transfected but not drug-treated wells) were pooled for each fluorescence channel and used to generate a two-dimensional reference data distribution. The two-dimensional data distribution of each individual well was then compared with the reference data distribution, and a KS value was calculated for each well. A heatmap based on two-dimensional KS values was then generated to aid the visualization of screening hits (Fig. 2). Using this methodology, we found that the average two-dimensional KS value for all untreated controls was 0.074. This indicated that the biological assay variation between controls was comparable with what would be predicted based on the algorithm described by Young (15), namely, a KS value of 0.077 denoting significant dissimilarity between populations, assuming significance on the $p = 0.05$ level and 1,000 objects analyzed in each sample population. By comparison, the average two-dimensional KS value for cells treated with the positive control, PAO, was 0.300.

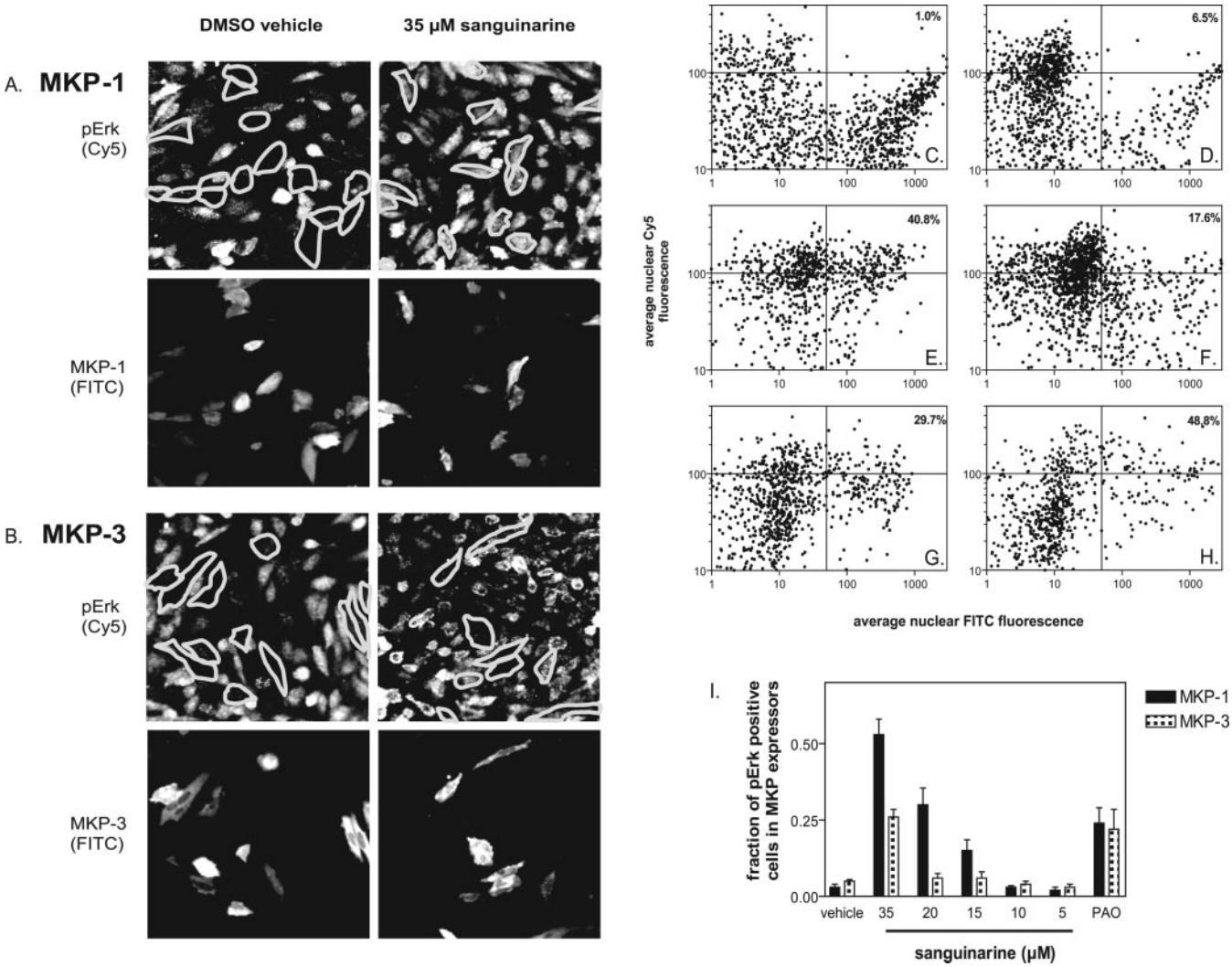

FIG. 5. **Sanguinarine inhibits MKP-1 but not MKP-3 in intact cells.** *A* and *B*, visual inspection of archived immunofluorescence images. MKP-expressing cells were visually identified from FITC channel images (*lower panels*), and their outlines were traced. Traces of MKP-positive cells were transferred onto phospho-ERK images (*upper panels*). *A*, in MKP-1 transfected cells, cells expressing MKP-1 have phospho-ERK levels comparable with that of surrounding cells not expressing MKP-1, indicating that sanguinarine (35 μM) inhibited ectopically expressed MKP-1. *B*, in MKP-3-transfected cells, MKP-3-expressing cells have lower levels of phospho-ERK than the surrounding non-expressing cells, indicating a lack of activity of sanguinarine on MKP-3. *C–H*, two-dimensional fluorescence plots of FITC (MKP) and Cy5 (pERK) intensities from selected wells. Cells were transfected with c-myc-MKP-1 (*C*, *E*, *G*) or c-myc-MKP-3 (*D*, *F*, *H*) and treated with TPA and vehicle (*C*, *D*), TPA and 35 μM sanguinarine (*E*, *F*), or TPA and PAO (*G*, *H*), and analyzed by HCS as described under "Materials and Methods." Both MKP-1- and MKP-3-transfected cells show a low percentage of phospho-ERK-positive cells in the MKP-expressing cell subpopulations (*upper right quadrants*). Sanguinarine increases the percentage of phospho-ERK-positive cells in MKP-1-expressing but not MKP-3-expressing cells. PAO, a nonspecific protein-tyrosine phosphatase inhibitor, increases the percentage of phospho-ERK-positive cells in both MKP-1 and MKP-3 expressors. Percentages shown in the *upper right-hand corners* are the fraction of pERK-positive cells in the MKP-expressing subpopulations. *I*, quantitative analysis of phospho-ERK-positive cells in MKP-expressing cell subpopulations. MKP expressors were defined by FITC staining intensity. A threshold for phospho-ERK-positive cells was established, and the percentage of pERK-positive cells in the MKP-expressing cells was calculated. Data are the averages from four independent experiments ± S.E.

TABLE I
Inhibition of dual specificity phosphatases by sanguinarine

	MKP-1 (CL100)[b]	MKP-L[b]	MKP-3[b]	Cdc25B[b]	PTP1B[c]	VHR[c]
	μM	μM	μM	μM	μM	μM
IC_{50}[a]	17.3 ± 1.2 (4)	12.5 ± 2.1 (7)	≫100 (4)	57.8 ± 11.6 (6)	67.9 ± 11.7 (6)	74.0 ± 5.3 (2)

[a] Average IC_{50} ± S.D. from (n) independent experiments.
[b] Full-length His-tagged protein.
[c] Full-length GST-tagged protein.

By selecting agents that showed a greater than 3-fold increase in two-dimensional KS values over the average of all data points, we identified six compounds (0.69% of total) as positives. Positive compounds from the screen were visually examined for restoration of phospho-ERK levels in MKP-1-expressing cells. Fig. 3 shows representative immunofluorescence images acquired in which MKP-1 expressing cells were identified on the basis of FITC fluorescence (*lower panels*) and mapped onto images acquired in the Cy5 channel (*top panels*). In the absence of small molecule compounds, MKP-1-expressing cells did not respond to TPA with increased ERK phosphorylation. Both the broad spectrum tyrosine phosphatase inhib-

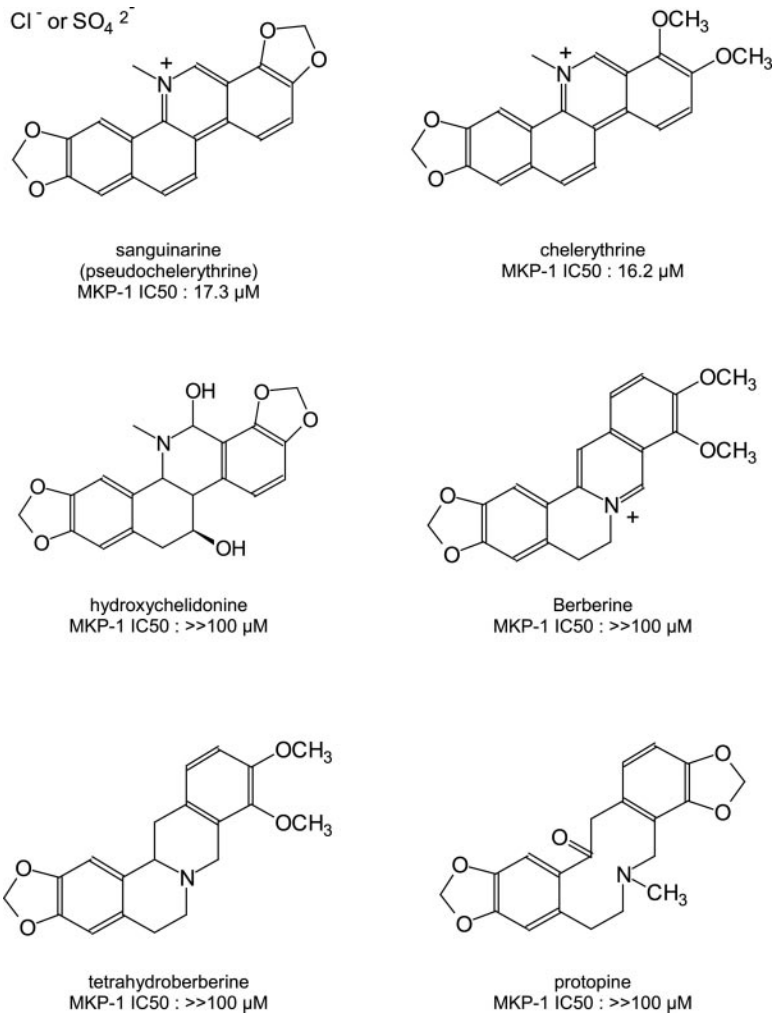

FIG. 6. **Structures of sanguinarine analogs.** The benzo[*c*]phenanthridine alkaloids, sanguinarine and chelerythrine, inhibited MKP-1 *in vitro*. Reduction of the benzo[*c*]phenanthridine aromatic ring system and hydroxylation abolished activity. Analogs containing the related dibenzo[*a*, *g*]quinolizine core structure were also devoid of MKP-1 inhibitory activity.

TABLE II
In vitro inhibition of MKP-1 and MKP-L by sanguinarine analogs

	MKP-1 (CL100) IC_{50}[a]	MKP-L IC_{50}[a]
	μM	*μM*
Sanguinarine	17.3 ± 1.2 (4)	12.5 ± 2.1 (7)
Tetrahydroberberine	≫100 (4)	≫100 (4)
Berberine	≫100 (4)	≫100 (4)
Protopine	≫100 (4)	≫100 (4)
chelerythrine	16.2 ± 1.7 (4)	26.3 ± 7.6 (4)
Hydroxychelidonine	≫100 (4)	≫100 (4)

[a] Average IC_{50} ± S.D. from (*n*) independent experiments

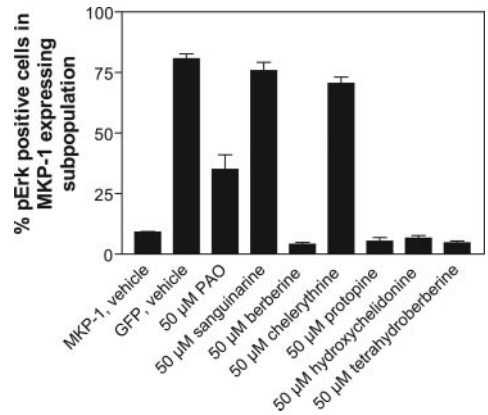

FIG. 7. **Inhibition of MKP-1 by sanguinarine analogs in intact cells.** The panel of sanguinarine analogs shown in Fig. 6 was analyzed for inhibition of ectopically expressed MKP-1 in HeLa cells using the chemical complementation assay. Cells expressing the phosphatase-inactive GFP were included as a negative control. Data are expressed as the percentage of pERK-positive cells in MKP-1 (GFP)-expressing subpopulations and are from a single experiment that has been repeated with identical results. Of the six compounds tested, only compounds with *in vitro* MKP-1 inhibitory activity, namely sanguinarine and chelerythrine, inhibited MKP-1 in intact cells.

itor, PAO, and the active compound in well E08 (sanguinarine) restored ERK phosphorylation in the MKP-1 expressing cells, confirming the results from the two-dimensional KS analysis. Treatment of MKP-1 transfected cells with sanguinarine resulted in a concentration-dependent increase of pERK-positive cells in the MKP-1-expressing cell subpopulations. When the data were normalized to the percentage of pERK-positive cells in GFP expressors, the concentration of sanguinarine required for a 50% effect (ED_{50}) was 10 μM (Fig. 4).

Sanguinarine Inhibits MKP-1 but Not MKP-3 in Intact Cells—To examine whether sanguinarine was selective for MKP-1 over the closely related MKP-3, HeLa cells were transfected with c-myc-tagged MKP-1 or MKP-3 and analyzed using the chemical complementation assay as described above. Immunofluorescence images taken in the FITC (Fig. 5, *A* and *B*, *bottom*) and Cy5 (Fig. 5, *A* and *B*, *top*) channels showed that both MKP-1 and MKP-3 reduced ERK phosphorylation in the MKP-expressing cells. Inclusion of sanguinarine (35 μM) restored ERK phosphorylation in MKP-1 expressors, but not in MKP-3 expressors (Fig. 5, *A* and *B*, *white traces*), indicating that sanguinarine inhibited MKP-1, but

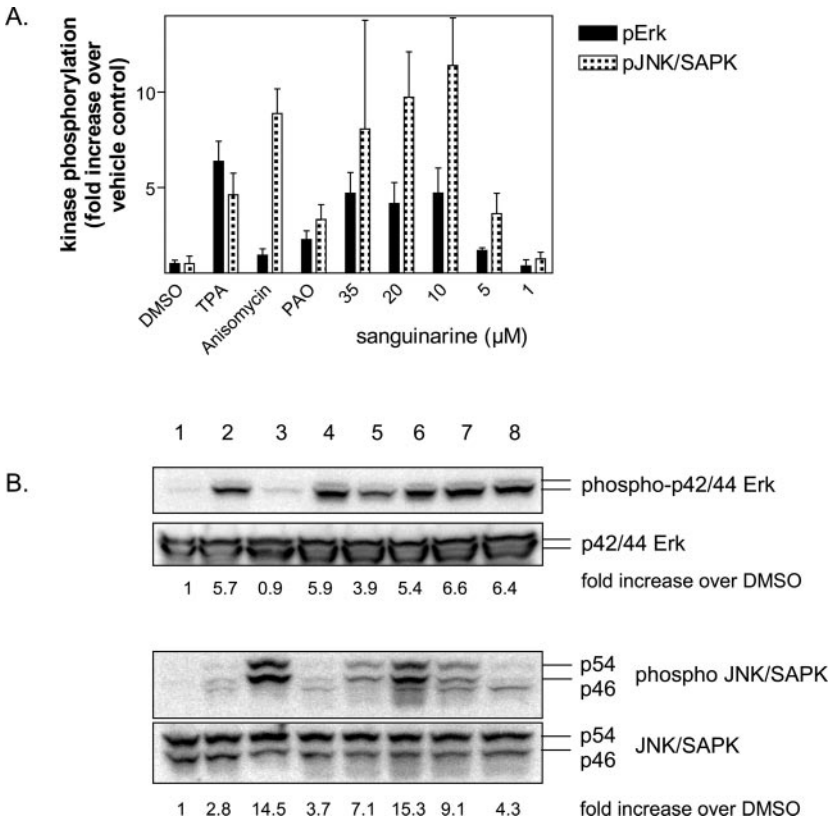

FIG. 8. **Sanguinarine induces phospho-ERK and phospho-JNK in PANC-1 cells.** *A*, immunofluorescence. PANC-1 cells were plated in the wells of a 384-well plate and treated for 30 min. with vehicle, TPA, anisomycin, PAO, or sanguinarine. Cells were simultaneously immunostained with phospho-ERK and phospho-JNK antibodies followed by AlexaFluor 488- and AlexaFluor 647-conjugated secondary antibodies and analyzed for nuclear phospho-ERK and phospho-JNK fluorescence intensities on the ArrayScan. Data were background-corrected for each treatment condition to account for potential compound autofluorescence, and the average nuclear pERK and pJNK fluorescence intensities from 1,000 individual cells/well were represented, normalized to vehicle control. Data are the averages from at least four independent experiments ± S.E. *B*, Western blot. Lysates from subconfluent monolayers of PANC-1 cells treated with vehicle or inhibitors were separated on SDS-PAGE and immunoblotted with anti-pERK, anti-ERK, anti-pJNK/SAPK, and anti JNK/SAPK antibodies. *Lane 1*, vehicle (Me_2SO (*DMSO*)); *lane 2*, 5 μM PAO; *lane 3*, 25 μg/ml anisomycin; *lane 4*, 500 ng/ml TPA; *lanes 5–8*, 5, 10, 20, and 35 μM sanguinarine, respectively. Band intensities were quantitated by luminometry and are presented as -fold increases over vehicle control of phospho-ERK and phospho-JNK levels, normalized to total ERK and JNK, respectively. Data are from a single experiment that has been repeated with similar results.

not MKP-3 in intact cells. Single cell two-dimensional fluorescence intensity plots indicated that both MKP-1 and MKP-3 caused a reduction of phospho-ERK-positive cells in both MKP-1 and MKP-3 expressors (Fig. 5, *C* and *D*). Treatment with sanguinarine increased the proportion of phospho-ERK-positive cells in the MKP-1 expressors (Fig. 5*E*) but did not affect MKP-3-expressing cells (Fig. 5*F*). In contrast, the broad spectrum protein-tyrosine phosphatase inhibitor, PAO, equally affected MKP-1- and MKP-3-expressing cells (Fig. 5, *G* and *H*). Quantitation of the fraction of cells above a phospho-ERK threshold demonstrated that sanguinarine substantially increased the fraction of phospho-ERK-positive cells in MKP-1, but not in MKP-3-expressing cell subpopulations, indicating that the compound selectively inhibited MKP-1 but not MKP-3 in intact cells. At the highest concentration tested (35 μM) sanguinarine started to show slight red autofluorescence, which possibly contributed to its apparent effect on phospho-ERK levels in MKP-3-expressing cells.

In Vitro Phosphatase Inhibition and Structure Activity Relationship Studies—We next examined the ability of sanguinarine to inhibit MKP-1 and related phosphatases *in vitro* and found it to be a potent and selective inhibitor of MKP-1 compared with MKP-3, VHR, Cdc25B, and protein-tyrosine phosphatase 1B (Table I). We then exploited the availability of sanguinarine analogs from commercial sources and obtained five additional compounds possessing a variety of alterations in the benzophenanthridine scaffold (Fig. 6). One

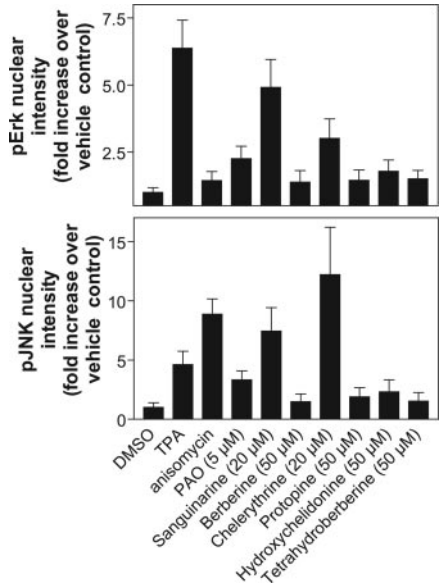

FIG. 9. **Compounds with MKP-1 inhibitory activity induce ERK and JNK phosphorylation in human pancreatic cancer cells.** PANC-1 cells were treated with sanguinarine or analogs for 30 min at the indicated concentrations and analyzed for pERK and pJNK levels by indirect immunofluorescence as described in the legend to Fig. 8. Data are the averages from at least four independent experiments ± S.E. *DMSO*, Me_2SO.

compound, chelerythrine, which is structurally similar to sanguinarine, was also found to be a micromolar inhibitor of MKP-1 (IC_{50} = 16.2 μM). More extensive modifications of the sanguinarine structure, such as hydroxylation and reduction of the phenanthridine scaffold or changing the core structure to the related dibenzo[*a*,*g*]quinolizine ring system, abolished MKP-1 inhibitory activity (Table II), suggesting that a planar aromatic ring system was required for MKP-1 inhibition. When analyzed for cellular inhibition of MKP-1, we found only sanguinarine and chelerythrine were active in the chemical complementation assay (Fig. 7), consistent with their *in vitro* MKP-1 inhibitory activities.

Compounds with MKP-1 Inhibitory Activity Induce ERK and JNK Phosphorylation in Human Pancreatic Cancer Cells—MKP-1 dephosphorylates ERK, JNK, and p38 (22). We therefore investigated the ability of putative MKP-1 inhibitors on the phosphorylation status of ERK and JNK/SAPK as a phenotypic readout consistent with MKP-1 inhibition. We chose PANC-1 human pancreatic cancer cells because they were shown to express high levels of MKP-1 (7). Fig. 8 shows that sanguinarine increased both phospho-ERK and phospho-JNK levels in PANC-1 cells, as measured by immunofluorescence and Western blot analysis. In contrast, sanguinarine analogs devoid of MKP-1 inhibitory activity failed to induce either phospho-ERK or phospho-JNK in PANC-1 cells (Fig. 9).

DISCUSSION

HCS provides a potentially powerful phenotypic method to identify small molecules with attractive cellular attributes. In our recently described current embodiment of an HCS approach (14), we found that 22 of the 720 natural product compounds analyzed (3.06%) caused a reduction in pERK subpopulation differences of ≥60% compared with the vehicle-treated control. A visual evaluation of archived images, however, revealed that only one compound, sanguinarine, unambiguously produced a phenotype in which c-myc-MKP-1-expressing cells had levels of phospho-ERK comparable with non-MKP-1-expressing cells (Fig. 3, *well E08*). Thus, a large number of false positives were identified with the previously described algorithm. By using two-dimensional KS values as the primary selection tool, we were able to apply a more stringent selection criterion and still readily preserve the most important natural product phosphatase inhibitor. The two-dimensional KS statistic reduced the number of false positives in the chemical complementation assay by 70% compared with our previously used method while still retaining the ability to detect the most active positive compound.

Sanguinarine is a bioactive alkaloid from the toxic plant *Chelidonium majus* (Greater Celandine), the extracts of which have long been used in traditional herbal medicine. The dried plant is currently monographed in the European Pharmacopoeia (23) as "*Chelidonii herba*" for the treatment of gastrointestinal disorders. Documented properties of sanguinarine include antiviral, antimicrobial, and even antitumor activity (reviewed in (24)).

Multiple cellular activities of sanguinarine have been reported, including inhibition of nuclear factor κB (25), suppression of vascular endothelial growth factor-induced angiogenesis (26), down-regulation of adhesion molecules (27), and cell cycle arrest in G_1/S and G_2/M (28), many of which occur at low or submicromolar concentrations. Despite the multitude of reports detailing the cellular activities of sanguinarine, however, a primary cellular target has not been identified. *In vitro*, sanguinarine has been reported to inhibit the catalytic subunit of PKA (IC_{50} = 6 μM) (29), monoamine oxidase (IC_{50} = 24.5 μM) (30), Na^+/K^+-ATPase (IC_{50} = 6.6 μM) (31), and to inhibit binding of colchicine and podophyllotoxin to tubulin (IC_{50} = 32 and 46 μM) (32). None of these *in vitro* targets, however, readily explain the cellular activities of sanguinarine, and to our knowledge, none of its *in vitro* activities have been translated into cellular activity. Interestingly, sanguinarine is essentially inactive against PKC (217 μM) (29), whereas the closely related chelerythrine has been reported as a potent (1 μM) inhibitor of this kinase. In contrast, both chelerythrine and sanguinarine have MKP-1 inhibitory activity. This suggests that the benzophenanthridine core structure is a pharmacophore with rich potential for structural and functional modifications.

Sanguinarine causes bimodal cell death (33). At lower concentrations (1–4 μM), cells treated with sanguinarine exhibit the typical signs of apoptosis. At higher concentrations, however (9 and 17 μM), signs of apoptosis are absent and cells die by an alternative mechanism termed oncosis (33), a form of cellular death characterized by cell swelling and surface blistering (34). Although apoptosis has been accepted as the predominant mechanism of drug-induced cell death in preclinical experimental models and in clinically sensitive tumors, drug-induced cell death can include other mechanisms (35). It is thought that alternative forms of cell death are important under conditions of impaired apoptotic response (36), thus, potentially contributing to chemoresistance. Consistent with this, sanguinarine was shown to sensitize human cervical cancer cells selected for cisplatin resistance (33). It is therefore possible that MKP-1 plays a role in oncosis.

In conclusion, we have discovered a new cellular target for an interesting bioactive compound that has long been known to possess a range of interesting biological activities including cytotoxicity. Our data illustrate the potential utility of an HCS assay to identify an inhibitor of MKP-1 that was selective for the related VHR, MKP-3, and $Cdc25B_2$ even from a relatively small number of compounds. The approach did not require the production of recombinant enzyme and allowed for an analysis of MKP-1 in its physiological content, eliminating the ambiguities associated with *in vitro* enzyme assays.

Acknowledgments—We thank Dr. Stephen Keyse and Dr. Zhong-Yin Zhang for providing CL100 and MKP-3 expression plasmids, Dr. Nicholas Tonks for the mammalian MKP-1 expression vector, Dr. Jack Dixon for a construct encoding His-tagged MKP-L, and Julian DeFranco for technical assistance.

REFERENCES

1. Sanchez-Perez, I., Martinez-Gomariz, M., Williams, D., Keyse, S. M., and Perona, R. (2000) *Oncogene* **19,** 5142–5152
2. Franklin, C. C., Srikanth, S., and Kraft, A. S. (1998) *Proc. Natl. Acad. Sci. U. S. A.* **95,** 3014–3019
3. Small, G. W., Shi, Y. Y., Edmund, N. A., Somasundaram, S., Moore, D. T., and Orlowski, R. Z. (2004) *Mol. Pharmacol.* **66,** 1478–1490
4. Magi-Galluzzi, C., Mishra, R., Fiorentino, M., Montironi, R., Yao, H., Capodieci, P., Wishnow, K., Kaplan, I., Stork, P. J., and Loda, M. (1997) *Lab. Investig.* **76,** 37–51
5. Bang, Y. J., Kwon, J. H., Kang, S. H., Kim, J. W., and Yang, Y. C. (1998) *Biochem. Biophys. Res. Commun.* **250,** 43–47
6. Wang, H., Cheng, Z., and Malbon, C. C. (2003) *Cancer Lett.* **191,** 229–237
7. Liao, Q., Guo, J., Kleeff, J., Zimmermann, A., Buchler, M. W., Korc, M., and Friess, H. (2003) *Gastroenterology* **124,** 1830–1845
8. Denkert, C., Schmitt, W. D., Berger, S., Reles, A., Pest, S., Siegert, A., Lichtenegger, W., Dietel, M., and Hauptmann, S. (2002) *Int. J. Cancer* **102,** 507–513
9. Loda, M., Capodieci, P., Mishra, R., Yao, H., Corless, C., Grigioni, W., Wang, Y., Magi-Galluzzi, C., and Stork, P. J. (1996) *Am. J. Pathol.* **149,** 1553–1564
10. Stewart, A. E., Dowd, S., Keyse, S. M., and McDonald, N. Q. (1999) *Nat. Struct. Biol.* **6,** 174–181
11. Camps, M., Nichols, A., Gillieron, C., Antonsson, B., Muda, M., Chabert, C., Boschert, U., and Arkinstall, S. (1998) *Science* **280,** 1262–1265
12. Giuliano, K. A., DeBiasio, R. L., Dunlay, T., Gough, A., Volosky, J. M., Zock, J., Pavlakis, G. N., and Taylor, D. L. (1997) *J. Biomol. Screen.* **2,** 249–259
13. Vogt, A., Takahito, A., Ducruet, A. P., Chesebrough, J., Nemoto, K., Carr, B. I., and Lazo, J. S. (2001) *J. Biol. Chem.* **276,** 20544–20550
14. Vogt, A., Cooley, K. A., Brisson, M., Tarpley, M. G., Wipf, P., and Lazo, J. S. (2003) *Chem. Biol.* **10,** 733–742
15. Young, I. T. (1977) *J. Histochem. Cytochem.* **25,** 935–941
16. Lampariello, F. (2000) *Cytometry* **39,** 179–188
17. Watson, J. V. (2001) *Cytometry* **43,** 55–68
18. Cox, C., Reeder, J. E., Robinson, R. D., Suppes, S. B., and Wheeless, L. L. (1988) *Cytometry* **9,** 291–298

19. Giuliano, K. A., Chen, Y. T., and Taylor, D. L. (2004) *J. Biomol. Screen.* **9,** 557–568
20. Peacock, J. A. (1983) *Monthly Notices of the Royal Astronomical Society* **202,** 615–627
21. Fasano, G., and Francescini, A. (1987) *Mon. Not. R. Astron. Soc.* **225,** 155–170
22. Chu, Y., Solski, P. A., Khosravi-Far, R., Der, C. J., and Kelly, K. (1996) *J. Biol. Chem.* **271,** 6497–6501
23. European Pharmacopoeia (2002) Vol. 4, pp. 2841–2842
24. Colombo, M. L., and Bosisio, E. (1996) *Pharmacol. Res.* **33,** 127–134
25. Chaturvedi, M. M., Kumar, A., Darnay, B. G., Chainy, G. B., Agarwal, S., and Aggarwal, B. B. (1997) *J. Biol. Chem.* **272,** 30129–30134
26. Eun, J. P., and Koh, G. Y. (2004) *Biochem. Biophys. Res. Commun.* **317,** 618–624
27. Tanaka, S., Sakata, Y., Morimoto, K., Tambe, Y., Watanabe, Y., Honda, G., Tabata, M., Oshima, T., Masuda, T., Umezawa, T., Shimada, M., Nagakura, N., Kamisako, W., Kashiwada, Y., and Ikeshiro, Y. (2001) *Planta Med.* **67,** 108–113
28. Adhami, V. M., Aziz, M. H., Reagan-Shaw, S. R., Nihal, M., Mukhtar, H., and Ahmad, N. (2004) *Mol. Cancer Ther.* **3,** 933–940
29. Wang, B. H., Lu, Z. X., and Polya, G. M. (1997) *Planta Med.* **63,** 494–498
30. Lee, S. S., Kai, M., and Lee, M. K. (2001) *Phytother. Res.* **15,** 167–169
31. Seifen, E., Adams, R. J., and Riemer, R. K. (1979) *Eur. J. Pharmacol.* **60,** 373–377
32. Wolff, J., and Knipling, L. (1993) *Biochemistry* **32,** 13334–13339
33. Ding, Z., Tang, S. C., Weerasinghe, P., Yang, X., Pater, A., and Liepins, A. (2002) *Biochem. Pharmacol.* **63,** 1415–1421
34. Majno, G., and Joris, I. (1995) *Am. J. Pathol.* **146,** 3–15
35. Houghton, J. A. (1999) *Curr. Opin. Oncol.* **11,** 475–481
36. Kitanaka, C., and Kuchino, Y. (1999) *Cell Death Differ.* **6,** 508–515
37. Groom, L. A., Sneddon, A. A., Alessi, D. R., Dowd, S., and Keyse, S. M. (1996) *EMBO J.* **15,** 3621–3632
38. Dowd, S., Sneddon, A. A., and Keyse, S. M. (1998) *J. Cell Sci.* **111,** 3389–3399
39. Press, W. H., Teukolsky, S. A., Vetterling, W. T., and Flannery, B. P. (1992) *Numerical Recipes in Fortran 77. The Art of Scientific Computing*, pp. 640–644, Cambridge University Press, Cambridge
40. Rice, R. L., Rusnak, J. M., Yokokawa, F., Yokokawa, S., Messner, D. J., Boynton, A. L., Wipf, P., and Lazo, J. S. (1997) *Biochemistry* **36,** 15965–15974
41. Lazo, J. S., Aslan, D. C., Southwick, E. C., Cooley, K. A., Ducruet, A. P., Joo, B., Vogt, A., and Wipf, P. (2001) *J. Med. Chem.* **44,** 4042–4049